Contrast agents for confocal microscopy: how simple chemicals affect confocal images of normal and cancer cells in suspension

Andrés F. Zuluaga
Rebekah Drezek
The University of Texas at Austin
Department of Electrical and Computer Engineering
Austin, Texas

Tom Collier
The University of Texas at Austin
The Biomedical Engineering Program
Austin, Texas

Reuben Lotan
The University of Texas M.D. Anderson Cancer Center
Department of Tumor Biology
Houston, Texas

Michele Follen
The University of Texas M.D. Anderson Cancer Center
Department of Gynecologic Oncology
Houston, Texas
     and
The University of Texas Health Science
     Center at Houston
Department of Obstetrics, Gynecology
     and Reproductive Sciences
Houston, Texas

Rebecca Richards-Kortum
The University of Texas at Austin
The Biomedical Engineering Program
Austin, Texas

Abstract. Normal and malignant human cervical cancer cells were imaged *in vivo* with confocal, phase contrast, and brightfield microscopies. Results were compared between cells in growth medium before and after addition of acetic acid, hypertonic saline solution, toluidine blue, and Lugol's iodine. The exogenous agents changed the backscattering characteristics of the cells when measured with confocal microscopy at 808 nm. A tendency toward higher scattering was observed in treated cells. Acetic acid and toluidine blue increased the brightness of the nucleus with respect to the cytoplasm in normal and cancer cells. Hypertonic saline solution made the cytoplasm brighter than the nucleus in both types of cells. The results indicate that simple chemicals can be used to enhance confocal microscopy's ability to differentiate intracellular components, such as nuclear size and shape. This can further confocal microscopy's ability to assess disease in cells and tissues. © *2002 Society of Photo-Optical Instrumentation Engineers.*
[DOI: 10.1117/1.1481047]

1 Introduction

Optical imaging techniques such as optical coherence tomography (OCT) and confocal microscopy are increasingly being applied to the real-time assessment of disease in tissue.[1–15] These techniques detect light that has been backscattered from tissue. While the source of backscattering from tissue is not fully understood, evidence suggests that differences in the index of refraction of intracellular components are a primary source of signal.[16–18] However these differences are small,[16–18] and allow only poor intracellular contrast. Agents that produced increased backscattering or improved image contrast could enhance the clinical utility of *in vivo* imaging techniques such as reflectance spectroscopy, OCT, and confocal microscopy.

Optical contrast agents are commonly used in clinical procedures. One example is colposcopy, where a physician examines the appearance of the cervix through a low power microscope. Exogenous chemicals are used to enhance the colposcopic visibility of precancerous and cancerous tissue. Acetic acid, hypertonic saline solution, toluidine blue, and iodine solutions have been shown to produce differential ef-

fects in the clinical appearance of normal and abnormal cervix as well as other organ sites.[19–33] Dyes used for photodynamic therapy have also recently been explored as contrast agents for use in detecting neoplasia.[34,35]

Here we present a study of the effects of these agents on confocal images of suspensions of normal cervical cells and cervical cancer cells. We find that these agents can enhance differences in the backscattering of nuclei of normal and cancer cells; thus they have the potential to improve image contrast and the ability to identify neoplasia *in vivo*.

2 Materials and Methods

Two types of human cervical cells were used in this study: normal cells from primary culture and an immortalized cancer cell line (SiHa line). The cells were imaged with confocal microscopy in growth medium and after the addition of four contrast agents: acetic acid, hypertonic saline, toluidine blue, and Lugol's iodine. Table 1 details the preparation of the contrast agents used. The cells were also imaged using phase contrast and transmitted light microscopy. Phase contrast microscopy was used to image cells before and after addition of

Address all correspondence to: Rebecca Richards-Kortum, PhD, ENS 610, The Biomedical Engineering Program, The University of Texas at Austin, Austin, TX 78712. Tel: (512) 471-2104; Fax: (512) 471-0616; E-mail: kortum@mail.utexas.edu

Table 1 Contrast agents and their preparations.

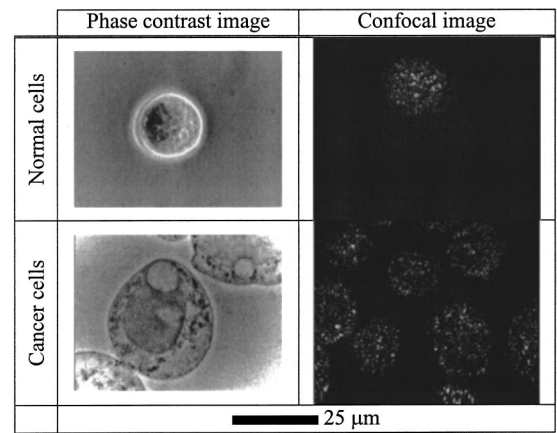| Contrast agent	Preparation
Acetic acid	6% (volume) glacial acetic acid in de-ionized water
Toluidine blue	1% (weight) toluidine blue O dye in de-ionized water
Hypertonic saline	840 mM phosphate buffered saline (6× physiologic concentration)
Lugol's iodine	5% iodine and 10% potassium iodine in de-ionized water

Fig. 1 Phase contrast and confocal images of normal and cancer cells in culture medium. The (common) scale bar in the bottom row is 25 μm wide.

acetic acid and hypertonic saline solution. Cells were imaged under transmitted light before and after the addition of toluidine blue and Lugol's iodine solution.

Normal and malignant human cervical epithelial cells were obtained from the lab of Dr. Reuben Lotan at the University of Texas M.D. Anderson Cancer Center in Houston. The cervical carcinoma cells (SiHa line) were obtained from the American Type Culture Collection (Rockville, MD). This cell line is HPV-16 (Human Papillomavirus-16) positive. SiHa cells were cultured in D–MEM (Dulbecco's modified eagle media) growth medium and Ham's F12 (GIBCO, Grand Island, NY) with supplements of 5% (vol/vol) fetal bovine serum (GIBCO) and antibiotics (100 units/mL penicillin and 100 mg/mL streptomycin). The normal cells were purchased from Clonetics (Walkersville, MD) and cultured through one passage in keratinocyte growth medium-2 (Clonetics). Routine checks for mycoplasma ensured that the cell cultures were free of contamination. After a brief incubation with 2 mM ethylenediamine-tetraacetic acid and 0.25% trypsin, the cultures were dispersed by repeated pipeting.

Four different samples of SiHa cells were obtained and imaged on four different days. A single sample of normal cells from one culture was obtained and imaged on a fifth day. Each day, images of available cells were obtained before and after the addition of each contrast agent. For confocal measurements, cell suspensions in growth medium were obtained in concentrations of 10^6 cells per milliliter. 20 μl aliquots were placed atop a layer of gelatin prepared in a Petri dish and imaged under a confocal microscope. The gelatin layer was necessary to reduce the specular reflectance from the bottom of the Petri dish, which would otherwise overwhelm the signal from the cells. The cells were then exposed to the same volume (20 μl) of one of the contrast agents chosen; the process was repeated starting with a fresh aliquot of cells for each of the agents. Identical methodology was followed for brightfield and phase contrast imaging of the cells, with the exception that the cell and contrast agent aliquots were placed on glass microscope slides.

Confocal images were obtained using a laser scanning confocal microscope at a wavelength of 808 nm. This instrument has been described in detail previously.[36] The field of view can be varied between 54×54 μm and 330×330 μm with a maximum lateral resolution of 0.8 μm. The depth resolution of the system was 2 μm.[36] Images were obtained at 15 frames per second. After acquisition, the images were converted to 8

bit grayscale values. Value 0 (black) corresponds to lowest reflectance and value 255 (white) corresponds to highest reflectance.

An estimate of the grayscale offset of the images was obtained after visual examination of all image histograms. Histogram stretching was used to enhance image contrast. For the images of normal cells, grayscale value 60 was reassigned to zero and grayscale values higher than 60 were evenly distributed along the entire 8 bit range (0–255). The images of the cancer cell line were similarly processed by shifting the value 30 to zero and evenly distributing the higher values along the 8-bit range. These differences in the zero level of the confocal images were attributed to normal drift in instrument performance. All subsequent analysis was done on the adjusted confocal images.

The cells were also imaged using bright-field and phase contrast microscopy to establish correlations between features of the confocal images and cell morphology. Images were digitized in color using a charge coupled device camera attached to the trinocular port of the microscope. The 24 bit, color images were converted to 8 bit grayscale images and were inverted before display. Thus, in the bright-field images, white corresponds to highest absorption (lowest transmission) and black to lowest absorption (highest transmission). All images were then appropriately adjusted to a common spatial scale.

3 Results

3.1 Cells in Growth Medium

Figure 1 shows confocal images of normal and cancer cells in growth medium. For comparison, the confocal images are shown alongside phase contrast images of the same cell sample. A scale bar 25 μm wide, common to all the images is shown at the bottom. The phase contrast images show the general morphology of the cells. The normal cell is round with an observed diameter of about 20 μm. The nucleus, the largest structure inside the cell, is seen as a dark structure about half the diameter of the cell, at the 10 o'clock position. Organelles are faintly observed in the cytoplasm. The cancer cells have a round shape, about 25 μm in diameter in this
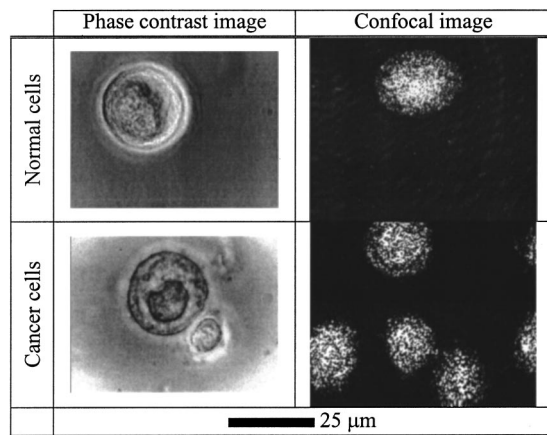
Fig. 2 Phase contrast and confocal images of normal and cancer cells after the addition of 6% acetic acid. Note the increased scattering and enhanced differentiation of the nucleus. The (common) scale bar in the bottom row is 25 μm wide.

Fig. 3 Phase contrast and confocal images of normal and cancer cells after the addition of hypertonic saline solution. Note the enhanced scattering from the cytoplasmic region resulting in negative nuclear contrast. The (common) scale bar in the bottom row is 25 μm wide.

image. Inside the cell membrane, a large number of organelles are observed as dark spots of varied diameters, distributed throughout the cytoplasm. The largest structure inside the cell is the nucleus.

The confocal image of the normal cell shows a single round cell about 20 μm in diameter. The nucleus is very faintly visible as a brighter region at the 2 o'clock position. The image of the cancer cells shows five full and at least four partial cells. The cells are round in shape and have diameters around 20 μm. The nucleus is most apparent in the largest fully imaged cell (lower right) at the 1−2 o'clock position. Noticeable background noise is observed as a series of thin vertical lines. The confocal images show very dim cells, with poorly defined outlines and very low nuclear-to-cytoplasmic contrast. To quantify these differences, average grayscale values were determined for representative nuclear, cytoplasmic, and background areas of images. Seven and ten cell images were sampled for the normal and cancer cell lines, respectively. For the confocal image of the normal cells the average values for cytoplasmic and nuclear images are 44.7 and 67.4, over a background level of 18.2. For the cancer (SiHa line) cells, the corresponding values are 24.0 for the cytoplasm (C), 28.0 for the nucleus (N), and 5.1 for the background (B).

3.2   Acetic Acid

Phase contrast and confocal images of cells exposed to 6% acetic acid are shown in Figure 2. The first row of images shows images of normal cells, and the second row shows images of cancer cells. The scale bar at the bottom, common to all images, is 25 μm wide. The phase contrast image of the normal cell exposed to acetic acid shows a round cell about 25 μm in diameter. The cell nucleus is seen as the single large structure inside the cell. The most interesting distinguishing feature of this image, with respect to the phase contrast image of the cells in growth medium, is the relative texture of the visible cell components, especially the nucleus. After the addition of acetic acid the components appear to have a rougher look. The phase contrast images of cancer cells show similar effects, especially in the nucleus. No change in the distribution of organelles in the cytoplasm is apparent.
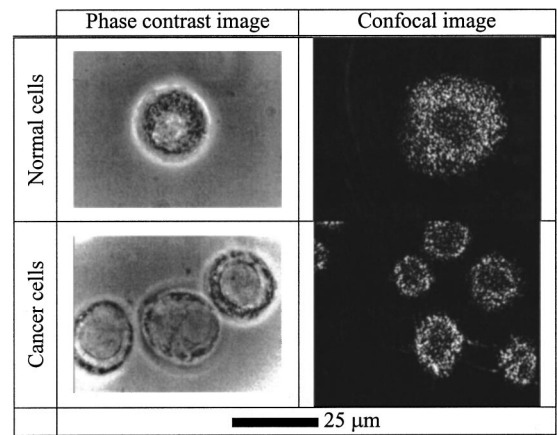
The confocal images after addition of acetic acid show a dramatic increase in the overall reflectance from the cells. The confocal image of the normal cell shows a cell about 25 μm in diameter with a much more apparent, brighter nuclear structure in the center 6 o'clock position of the cell. The nucleus appears to have a diameter two-thirds that of the cell, in good agreement with the corresponding phase contrast image. Like the normal cells, the cancer cells show greater overall scattering and nuclear differentiation in the confocal image. Almost four full cancer cells, all with similar characteristics, are seen in the image. The average grayscale values of five normal cells are: 64.6 (C) and 186.8 (N), with a background of 18.6. The values for ten cancer cells are 52.9 (C), 175.2 (N), and 5.1 (B).

3.3   Hypertonic Saline

Phase contrast and confocal images of cells exposed to hypertonic saline solution are shown in Figure 3. The phase contrast images here show an interesting change in the distribution of organelles inside the cell. The phase contrast image of the normal cell shows that organelles have migrated to the edge of the cell, leaving a lighter, more uniform void in the center probably containing the nucleus. In the phase contrast image of the cancer cells, almost all of the small organelles have moved toward the cell membrane. No other changes are observed in the nuclei or overall cell structure. The shapes and sizes of the cells and their nuclei are similar to those observed in the cells in growth medium alone.

The confocal images of the cells exposed to hypertonic saline solution show increased overall scattering and outline differentiation. They show higher nuclear-to-cytoplasmic contrast, but in these images nuclei appear darker than the surrounding cytoplasm. The average grayscale values for these images are: 84.74 (C), 50.45 (N), and 8.88 (B) for five normal cells; and 90.05 (C), 46.14 (N), and 4.82 (B) for ten cancer cells.

3.4   Toluidine Blue

Figure 4 shows bright-field and confocal images of the normal and cancer cells after the addition of 1% toluidine blue solu-
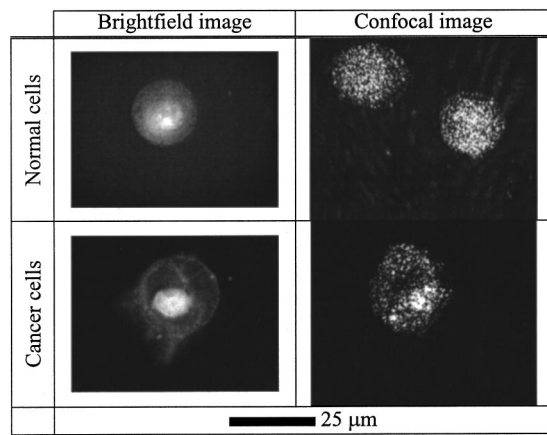
Fig. 4 Bright-field and confocal images of normal and cancer cells after the addition of 1% toluidine blue solution. The (common) scale bar in the bottom row is 25 μm wide.

Fig. 5 Bright-field and confocal images of normal and cancer cells after the addition of Lugol's iodine solution. Note the overall increase in scattering from the cell. The (common) scale bar in the bottom row is 25 μm wide.

tion. The inverted bright-field images show that the solution permeates the whole cell, although it concentrates in the nucleus. This is shown by the brighter regions of the image, which correspond to higher absorption. The cytoplasmic region of the normal cell shows relative uniformity in the measured absorption. The uptake of solution in the nucleus appears more uneven, with appreciable hot spots. Toluidine blue uptake in the cytoplasm of the cancer cell is not as uniform and appears to be slightly higher in the cell membrane and several filament-like regions inside the cytoplasm. The nucleus also exhibits bright spots. No morphologic changes were evident in any of the cells.

The confocal images of cells after the addition of toluidine blue show higher overall scattering and increased nuclear-to-cytoplasmic contrast. This is illustrated in the image of the normal cells, although the differentiation of nucleus and cytoplasm is not as high as in the cancer cells. In the image of the cancer cell, the nuclear region is located at the 4 o'clock position, and the differentiation is most evident. This image shows average grayscale values of 25.79 (C), 93.45 (N), and 5.13 (B) for ten images. The corresponding values for five images of the normal cell are 57.47 (C), 138.27 (N), and 21.14 (B).

3.5 Lugol's Iodine

Shown in Figure 5 are bright-field and confocal images of normal and cancer cells after the addition of Lugol's iodine. The inverted, bright-field images show regions of higher solution uptake in lighter shades of gray. The image of a normal cell shows a round cell about 20 μm in diameter with relatively uniform uptake of Lugol's iodine solution throughout the cell. The nucleus is distinguishable in the center of the cell and appears slightly brighter than the cytoplasm, especially around the edges. The bright-field image of the cancer cell shows slight uptake of the solution. Absorption is uniform throughout the cytoplasmic region of the cell and slightly lower in the nuclear region. This cell is also round in shape and 25 μm in diameter.

The confocal images of the cells show greater scattering than those of the cells in growth medium alone, giving better outline definition. However, the treated cells show little in-
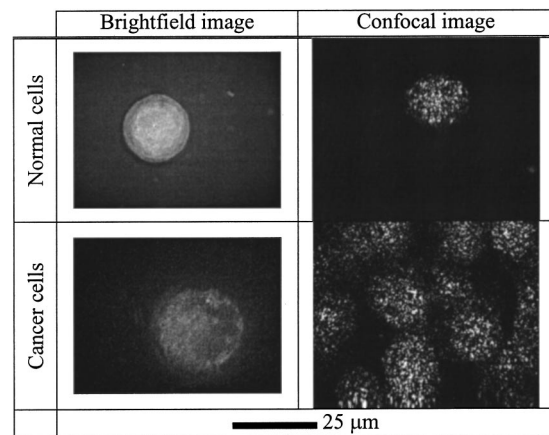
crease in the differentiation of intracellular structures. Both the normal and cancer cells appear of fairly uniform brightness. A structure, probably nuclear, is represented by slightly increased backscatter in the confocal image of the normal cell at the 7 o'clock position. The average intensity values for these images are: 80.26 (C), 144.67 (N), and 17.53 (B) for five confocal images of normal cells; and 50.18 (C), 95.33 (N), and 8.98 (B) for ten images of cancer cells.

3.6 Discussion and Conclusions

All of the contrast agents studied had an effect on the backscattering properties of cells, as viewed under reflectance confocal microscopy at 808 nm. In general, the addition of any of the agents resulted in increased backscattering from the cells and, in some cases, from different intracellular components. The results are summarized in Figure 6. Figure 6(a) shows the average grayscale values for representative regions of the confocal images of normal cells before and after the application of contrast agents. The error bars correspond to ± 1 standard deviation. The normal cells in growth medium have nuclei that are slightly brighter on average than the cytoplasm. Adding acetic acid, toluidine blue, and Lugol's iodine to normal cells increases the brightness of both the nucleus and cytoplasm. The relative differences between nucleus and cytoplasm are accentuated by acetic acid and toluidine blue. Toluidine blue and Lugol's iodine also increase the variability of the measurements, as evidenced by the larger standard deviations. Hypertonic saline solution makes the cytoplasm brighter than the nucleus in normal cells. The average brightness is changed the least by this agent.

Figure 6(b) shows the corresponding data for the cancer cells. Cancer cells in growth medium have almost identical brightness in the nucleus and cytoplasm. As with normal cells, acetic acid, toluidine blue, and Lugol's iodine increase the overall scattering of the cells. At the same time, acetic acid and toluidine blue enhance the differentiation between the nucleus and cytoplasm within the cells by making the nucleus substantially brighter than the cytoplasm. An increase in the variability of the measurements is observed with toluidine blue and Lugol's iodine. Hypertonic saline solution increases
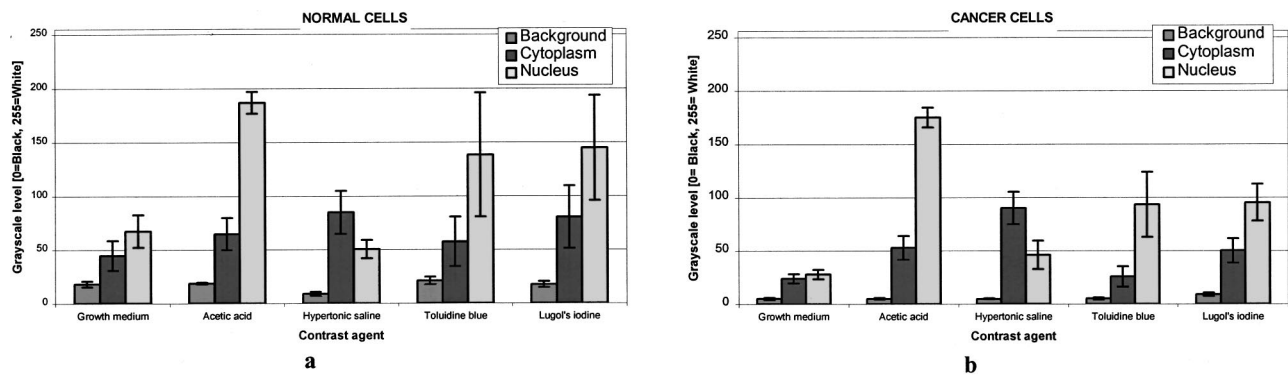
Fig. 6 (a) Average grayscale levels for representative segments of the confocal images of normal cells (seven images for growth medium, five images for each contrast agent). (b) Corresponding grayscale levels for the images of the cancer cells (ten images in all cases). The error bars correspond to ± one standard deviation.

the overall brightness of cancer cell images. However, this contrast agent causes the cytoplasm to be brighter than the nucleus.

Because they increase the relative difference between the nucleus and cytoplasm of cells, acetic acid, hypertonic saline, and toluidine blue appear to be the most promising of the studied chemicals. These contrast agents could enhance the ability to assess nuclear size and shape using *in vivo* confocal microscopy. Hypertonic saline solution has a dramatic effect on the cells in suspension. However, it is unclear whether a similar change can be expected in tissue samples, where cells are completely surrounded by other cells rather than by the contrast agent. This very likely reduces the chance of observing organelles migrating uniformly to the cell membrane, resulting in no improvement in the ability to accurately determine nuclear size one of the main features differentiating normal and abnormal cells.

The source of changes in the appearance of the confocal images is likely related to changes in the refractive index profile of the cell. The phase contrast images presented here provide a qualitative assessment of refractive index changes. Barer suggested a quantitative technique to measure changes in the refractive index based on index matching.[37] This approach has been successfully used to characterize epithelial cell refractive index.[38] In the future we will explore how contrast agents quantitatively change this refractive index profile.

It should be pointed out that live normal and abnormal cells and tissues may have different uptake ratios for all of these chemicals, and this may further the ability of confocal microscopy to assess changes in cells and tissue. Furthermore, custom-made molecular agents, such as photodynamic therapy drugs, which are preferentially taken up and retained by cancer cells may also be useful in enhancing the diagnostic ability of *in vivo* confocal microscopy.

Acknowledgments

References

1. M. Rajadhyaksha, M. Grossman, D. Esterwitz, R. Webb, and R. Anderson, "In-vivo confocal scanning laser microscope of human skin: melanin provides strong contrast," *J. Invest. Dermatol.* **104**, 946–952 (1995).

2. S. A. Boppart, G. J. Tearney, B. E. Bouma, J. F. Southern, M. E. Brezinski, and J. G. Fujimoto, "Noninvasive assessment of the developing Xenopus cardiovascular system using optical coherence tomography," *Proc. Natl. Acad. Sci. U.S.A.* **94**, 4256–4261 (1997).

3. A. M. Sergeev, V. M. Gelikonov, G. V. Gelikonov, F. I. Feldchtein, R. V. Kuranov, N. D. Gladkova, N. M. Shakhova, L. B. Snopova, A. V. Shakov, I. A. Kuznetzova, A. N. Denisenko, V. V. Pochinko, Y. P. Chumakov, and O. S. Streltzova, "In-vivo Endoscopic OCT Imaging of Precancer and Cancer States of Human Mucosa," *Opt. Express* **1**, 432–440 (1997).

4. M. E. Brezinski, G. J. Tearney, B. Bouma, S. A. Boppart, C. Pitris, J. F. Southern, and J. G. Fujimoto, "Optical biopsy with optical coherence tomography," *Ann. N.Y. Acad. Sci.* **838**, 68–74 (1998).

5. F. I. Feldchtein, G. V. Gelikonov, V. M. Gelikonov, R. V. Kuranov, A. M. Sergeev, N. D. Gladkova, A. V. Shakhov, N. M. Shakhova, L. B. Snopova, T. e. A.B., E. V. Zagainova, Y. P. Chumakov, and I. A. Kuznetzova, "Endoscopic applications of optical coherence tomography," *Opt. Express* **3**, 257–270 (1998).

6. M. Bohnke and B. R. Masters, "Confocal microscopy of the cornea [Review]," *Prog. Retinal Res.* **18**, 553–628 (1999).

7. B. E. Bouma and G. J. Tearney, "Power-efficient nonreciprocal interferometer and linear-scanning fiber-optic catheter for optical coherence tomography," *Opt. Lett.* **24**, 531–533 (1999).

8. J. F. de Boer, T. E. Milner, and J. S. Nelson, "Determination of the depth-resolved Stokes parameters of light backscattered form turbid media by use of polarization-sensitive optical coherence tomography," *Opt. Lett.* **24**, 300–302 (1999).

9. W. Hsing-Wen, J. Willis, M. J. F. Canto, M. V. Sivak, Jr., and J. A. Izatt, "Quantitative laser scanning confocal autofluorescence microscopy of normal, premalignant, and malignant colonic tissues," *IEEE Trans. Biomed. Eng.* **46**, 1246–1252 (1999).

10. C. Pitris, A. Goodman, S. Boppart, J. Libus, J. G. Fujimoto, and M. E. Brezinski, "High resolution imaging of gynecologic neoplasms using optical coherence tomography," *Obstetrics and Gynecology* **93**, 135–139 (1999).

11. M. Rajadhyaksha, S. Gonzalez, J. M. Zavislan, R. R. Anderson, and R. H. Webb, "In vivo confocal scanning laser microscopy of human skin II: advances in instrumentation and comparison with histology," *J. Invest. Dermatol.* **113**, 293–303 (1999).

12. A. M. Rollins, R. Ung-arunyawee, A. Chak, R. C. K. Wong, K. Kobayashi, M. V. Sivak, Jr., and J. A. Izatt, "Real-time in vivo imaging of human gastrointestinal ultrastructure by use of endoscopic optical coherence tomography with a novel efficient interferometer design," *Opt. Lett.* **24**, 1358–1360 (1999).

13. M. Tanifuji, M. Fukuda, and K. Tsunoda, "Functional imaging of the brain by using light," *Oyo Butsuri* **68**, 997–1007 (1999).

14. R. A. Drezek, T. Collier, C. K. Brookner, A. Malpica, R. Lotan, R. R. Richards-Kortum, and M. Follen, "Laser scanning confocal microscopy of cervical tissue before and after application of acetic acid," *Am. J. Obstetrics and Gynecology* **182**, 1135–1139 (2000).

15. R. M. Zucker, A. P. Keshaviah, O. T. Price, and J. M. Goldman,

"Confocal laser scanning microscopy of rat follicle development," *J. Histochem. Cytochem.* **48**, 781–791 (2000).

16. A. Dunn and R. Richards-Kortum, "Three-dimensional computation of light scattering from cells," *IEEE J. Sel. Top. Quantum Electron.* **2**, 898–905 (1997).

17. A. Sergeev, N. Gladkova, F. Feldchtein, V. Gelikonov, G. Gelikonov, L. Snopova, J. Ioannovich, K. Frangia, T. Pirza, I. Antoniu, A. Dunn, and R. Richards-Kortum, "Melanin effect on light scattering in tissues: from electrodynamics of living cell to OCT imaging," presented at SPIE Conference on Coherence Domain Optical Methods in Biomedical Science and Clinical Applications, 1997.

18. R. A. Drezek, A. Dunn, and R. Richards-Kortum, "Finite difference time domain modeling and goniometric measurements of light scattering form cells," *Appl. Opt.* **38**, 3651–3661 (1999).

19. R. Schultz and H. Skelton, "Value of acetic acid screening for flat genital condlyomata in men," *J. Urol. (Baltimore)* **139**, 777–779 (1988).

20. S. Silverman, Jr. "Early diagnosis of oral cancer," *Cancer (N.Y.)* **62**, 1796–1799 (1988).

21. G. Fiscor, S. Fuller, J. Jeromin, D. Beyer, and F. Janca, "Enhancing cervical cancer detection using nucleic acid hybridization and acetic acid tests," *Nurse Practitioner* **15**, 26–30 (1990).

22. L. Van Le, F. Broekhuizen, R. Janzer-Steele, M. Behar, and T. Samter, "Acetic acid visualization of the cervix to detect cervical dysplasia," *Obstetrics and Gynecology* **81**, 293–295 (1993).

23. J. Liu, Q. Wang, B. Li, X. Meng, Y. Zhang, X. Du, J. Yan, Y. Ping, and W. Li, "Superficial carcinomas of the esophagus and gastric cardia. A clinicopathological analysis of 141 cases," *Chin. Med. J.* **108**, 754–759 (1995).

24. R. H. Riddell, "Early detection of neoplasia of the esophagus and gastroesophageal junction," *Am. J. Gastroenterology* **91**, 853–863 (1996).

25. V. Meyer, P. Burtin, P. Bour, A. Blanchi, P. Cales, F. Oberti, B. Person, A. Croue, S. Dohn, R. Benoit, B. Fabiani, and J. Boyer, "Endoscopic detection of early esophageal cancer in a high-risk population: does Lugol staining improve videoendoscopy?," *Gastrointestinal Endoscopy* **45**, 480–484 (1997).

26. M. Derenzini, D. Trere, A. Pession, L. Montanaro, V. Sirri, and R. L. Ochs, "Nucleolar function and size in cancer cells," *Am. J. Pathol.* **152**, 1291–1297 (1998).

27. I. C. Martin, C. J. Kerawala, and M. Reed, "The application of toluidine blue as a diagnostic adjunct in the detection of epithelial dysplasia," *Oral Surgery, Oral Medicine, Oral Pathology Oral Radiology and Endodontics* **85**, 444–446 (1998).

28. Y. Nakanishi, A. Ochiai, K. Yoshimura, H. Kato, T. Shimoda, H. Yamaguchi, Y. Tachimori, H. Watanabe, and S. Hirohashi, "The clinicopathologic significance of small areas unstained by Lugol's iodine in the mucosa surrounding resected esophageal carcinoma: an analysis of 147 cases," *Cancer (N.Y.)* **82**, 1454–1459 (1998).

29. J. B. Epstein and C. Scully, "Assessing the patient at risk for oral squamous cell carcinoma," *Special Care in Dentistry* **17**, 120–128 (1997).

30. J. B. Epstein, C. Oakley, A. Millner, S. Emerton, E. van der Meij, and N. Le, "The utility of toluidine blue application as a diagnostic aid in patients previously treated for upper oropharyngeal carcinoma," *Oral Surgery, Oral Medicine, Oral Pathology Oral Radiology and Endodontics* **83**, 537–547 (1997).

31. A. N. Kurniawan and L. S. Handikin, "Some experience with in vivo staining of early laryngeal cancer in Jakarta, Indonesia," *Cancer Detection and Prevention* **4**, 313–317 (1981).

32. Y. Nakanishi, A. Ochiai, T. Shimoda, H. Yamaguchi, Y. Tachimori, H. Kato, H. Watanabe, and S. Hirohashi, "Epidermization in the esophageal mucosa: unusual epithelial changes clearly detected by Lugol's staining," *Am. J. Surgical Pathology* **21**, 605–609 (1997).

33. E. M. Chisholm, S. R. Williams, J. W. Leung, S. C. Chung, C. A. van Hasselt, and A. K. Li, "Lugol's iodine dye-enhanced endoscopy in patients with cancer of the oesophagus and head and neck," *Eur. J. Surgical Oncology* **18**, 550–552 (1992).

34. C. Fritsch, K. Lang, W. Neuse, T. Ruzicka, and P. Lehmann, "Photodynamic diagnosis and therapy in dermatology," *Skin Pharmacology Applied Skin Physiology* **11**, 358–373 (1998).

35. S. Lam, "Bronchoscopic, photodynamic, and laser diagnosis and therapy of lung neoplasms," *Curr. Opin. in Pulmonary Medicine* **2**, 271–276 (1996).

36. C. Smithpeter, A. Duan, R. Drezek, T. Collier, and R. Richards-Kortum, "Near real time confocal microscopy of cultured amelanotic cells: sources of signal, contrast agents and limits of contrast," *J. Biomed. Opt.* **3**, 429–436 (1998).

37. R. Barer, "Refractometry and Interferometry of Living Cells," *J. Opt. Soc. Am.* **47**, 545–556 (1957).

38. R. Drezek, A. Dunn, and R. Richards-Kortum, "Light scattering from cells: finite-difference time-domain simulations and goniometric measurements," *Appl. Opt.* **38**, 3651–3661 (1999).